

Higgs Oscillations in a Unitary Fermi SuperfluidP. Dyke¹, S. Musolino², H. Kurkjian³, D. J. M. Ahmed-Braun⁴, A. Pennings¹, I. Herrera¹, S. Hoinka¹, S. J. J. M. F. Kokkelmans⁴, V. E. Colussi^{5,6} and C. J. Vale^{1,7}¹*Optical Sciences Centre, ARC Centre of Excellence in Future Low-Energy Electronics Technologies, Swinburne University of Technology, Melbourne, Victoria 3122, Australia*²*Université Côte d'Azur, CNRS, Institut de Physique de Nice, 06200 Nice, France*³*Laboratoire de Physique Théorique, Université de Toulouse, CNRS, UPS, France*⁴*Eindhoven University of Technology, P.O. Box 513, 5600 MB Eindhoven, The Netherlands*⁵*Pitaevskii BEC Center, CNR-INO and Dipartimento di Fisica, Università di Trento, 38123 Trento, Italy*⁶*Infleqtion, Inc., 3030 Sterling Circle, Boulder, Colorado 80301, USA*⁷*CSIRO, Research Way, Clayton, Victoria 3168, Australia* (Received 13 November 2023; revised 13 February 2024; accepted 25 March 2024; published 30 May 2024)

Symmetry-breaking phase transitions are central to our understanding of states of matter. When a continuous symmetry is spontaneously broken, new excitations appear that are tied to fluctuations of the order parameter. In superconductors and fermionic superfluids, the phase and amplitude can fluctuate independently, giving rise to two distinct collective branches. However, amplitude fluctuations are difficult to both generate and measure, as they do not couple directly to the density of fermions and have only been observed indirectly to date. Here, we excite amplitude oscillations in an atomic Fermi gas with resonant interactions by an interaction quench. Exploiting the sensitivity of Bragg spectroscopy to the amplitude of the order parameter, we measure the time-resolved response of the atom cloud, directly revealing amplitude oscillations at twice the frequency of the gap. The magnitude of the oscillatory response shows a strong temperature dependence, and the oscillations appear to decay faster than predicted by time-dependent Bardeen-Cooper-Schrieffer theory applied to our experimental setup.

DOI: [10.1103/PhysRevLett.132.223402](https://doi.org/10.1103/PhysRevLett.132.223402)

The ability of interacting particles to act collectively underpins many of the remarkable properties of quantum matter. From superfluidity and superconductivity to magnetism and elementary particles, order parameters and their fluctuations govern a wide variety of collective quantum phenomena [1]. Phase transitions characterized by a complex bosonic order parameter are generally accompanied by the emergence of two distinct collective excitations. Phase fluctuations that manifest as sound waves in neutral systems [2] become massive in the presence of long-range interactions [3,4], while amplitude (or strictly speaking modulus) fluctuations are always gapped. This behavior is reminiscent of the Higgs field [5] in high-energy physics, whose phase is responsible for mass acquisition via the Anderson-Higgs mechanism and whose amplitude gives rise to the Higgs boson. The analogy relies on the iconic “Mexican hat” potential [6,7], governing the dynamics of these complex bosonic fields. Among the systems where an effective action with this form emerges in nonrelativistic matter are Bose gases near the superfluid-Mott insulator transition [8,9], spinor Bose-Einstein condensates (BECs) [10], atoms in optical cavities [11], dipolar gases in the supersolid phase [12], and antiferromagnetic materials [13].

The analogy with the Higgs field is often extended to the order parameter Δ of fermionic pair condensates [14–16].

This case, however, is more subtle as the dynamics of $|\Delta|$ result from (pair-breaking) biexcitations of the fermionic quasiparticles. Unlike phase fluctuations, which obey superfluid hydrodynamics [17], amplitude fluctuations *cannot* be modeled by a low-energy effective action such as the Mexican hat potential [18] and remain an intrinsically many-body phenomenon, with unique phenomenology.

The microscopic description of a Bardeen-Cooper-Schrieffer (BCS) superconductor and/or superfluid shows that there exists a collective amplitude mode within the pair-breaking continuum [19], which persists even in presence of amplitude-phase coupling [20]. In the zero-momentum limit, the spectral weight of the amplitude mode vanishes, yet amplitude *oscillations* still occur due to the presence of a nonanalytic singularity in the amplitude response function. Within a mean-field approximation, the frequency of these amplitude oscillations is set at twice the gap in the fermionic excitation spectrum [21], and the oscillations decay according to a power law with an exponent that changes at the transition from BCS to the BEC regime [22–26]. In the regime of nonlinear excitations, other asymptotic behaviors become possible, including persistent oscillations [27–29].

Nonlinear amplitude oscillations have been recorded through third harmonic generation in BCS [14] and cuprate

[30,31] superconductors, and a dressed amplitude mode has been observed in charge density wave [32–34] superconductors. The case of neutral Fermi gases is *a priori* favorable since the strength $|\Delta|$ of the pair condensate can be accessed directly, either by tuning the interaction strength [35] or via radio-frequency coupling to a third internal state [36]. To date, a broad spectroscopic peak was reported around the threshold of the pair-breaking continuum [16,35], but the spectral resolution was too low to unambiguously identify the singularity responsible for amplitude oscillations. Modulated interactions have previously been used to study the dynamics of pair condensation [37–39].

Here, we directly observe amplitude oscillations in an ultracold atomic Fermi condensate with resonant interactions. We excite the oscillations by a uniform (zero-momentum) quench of the interactions using a magnetic Feshbach resonance. We probe the ensuing out-of-equilibrium dynamics using high-momentum Bragg scattering, tuned to resonantly excite condensed pairs, which is highly sensitive to variations of the order parameter. Our real-time experiment allows us to characterize the frequency, magnitude, and decay of the oscillations. Compared to predictions from time-dependent BCS theory, our experiment confirms oscillations occur at twice the gap (2Δ) and show qualitative agreement on the temperature dependence of the oscillation magnitude, with a reduction as the number of condensed pairs decreases near the critical temperature T_c [22]. The observed oscillations at unitarity decay faster than predicted by BCS theory, even when experimental effects such as inhomogeneous broadening are taken into account.

Our experimental protocol is depicted in Fig. 1 [21]. An ultracold gas of fermionic ${}^6\text{Li}$ atoms is prepared in a balanced mixture of two spin states, initially at thermal equilibrium. Elastic collisions between atoms in these states can be tuned by an external magnetic field through a broad Feshbach resonance [40]. Interactions are characterized by the dimensionless parameter $1/(k_F a)$ where $k_F = (3\pi^2 n)^{1/3}$ is the Fermi wave vector, n is the atomic density, and a is the s -wave scattering length. The cloud is initially prepared below T_c , slightly to the BCS side of the Feshbach resonance [$1/(k_F a_i) \approx -0.18 \pm 0.02$]. The magnetic field is then ramped to unitarity (where $a \rightarrow \infty$) in a time $t_q = 50 \mu\text{s}$, too fast for the system to follow adiabatically, creating a superposition of the more strongly paired ground state and the continuum of excited states. As this superposition evolves, the pairing field oscillates at a frequency set by the energy difference between the ground and excited states, leading to Higgs oscillations of the order parameter.

According to Refs. [22,24,27] a power-law damping of the oscillations occurs, due to the spread in energy of the lowest-lying excited states. In the BCS (weak-coupling) limit, the lowest energy excitations occur at the Fermi surface, $p \approx \hbar k_F$, where the 3D density of excited states is

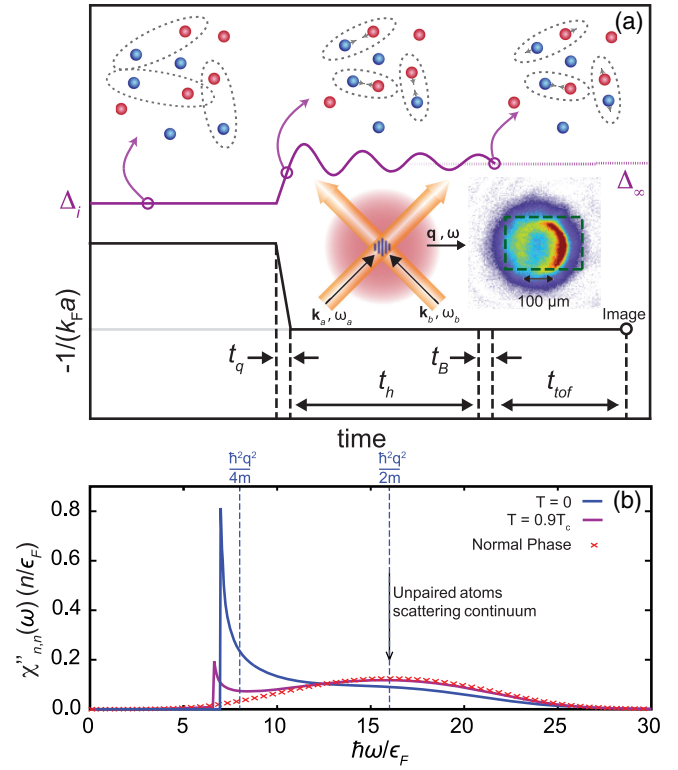


FIG. 1. Excitation and detection of amplitude oscillations in a paired Fermi superfluid. (a) Pairs of fermions (dashed ellipses) initially at equilibrium are excited by a rapid variation of the interatomic interactions in a time $t_q = 50 \mu\text{s}$. After a variable hold time t_h , we measure the Bragg response of the nearly uniform central region. The momentum imparted by the pulse is accessed through the center-of-mass displacement in time-of-flight images (see Supplemental Material [40]). The quench projects the pairs into a superposition of the more tightly bound ground state and the continuum of fermionic biexcitations, with energies $2\epsilon_k$. The pairing field thus begins oscillating, triggering oscillations of the order parameter (purple curve). The continuum edge at $2\Delta \equiv 2\min_k(\epsilon_k)$ sets the frequency of the oscillations, which attenuate over time due to the spread of the excited state wave function over energies $2\epsilon_k$, eventually stabilizing at Δ_∞ . At nonzero temperatures, the superfluid pairs are surrounded by a thermal cloud of unpaired atoms (isolated blue and red dots), reducing the spectral weight of the amplitude oscillations. (b) The imaginary part of the density-density response function in the random-phase approximation and for the large pair center-of-mass momentum q used in our Bragg spectroscopy. The energy and magnitude of the peak at the dissociation threshold $\hbar\omega_{\text{th}} = \sqrt{4\Delta^2 + (\hbar^2 q^2/4m - \mu)^2}$ varies with Δ during the postquench evolution, which makes our Bragg measurement sensitive to the amplitude oscillations.

large, and this small spread in energy leads to oscillations decaying slowly, as $t^{-1/2}$ [22]. In the opposite limit of tightly bound molecules, the dispersion minimum occurs at $p = 0$, where the density of states vanishes, as for free particles. The evolution of the excited wave function is thus similar to a 3D ballistic expansion and the overlap with the molecular ground state decays as $t^{-3/2}$ [24].

We model these dynamics using time-dependent BCS theory [67]. The initial state of the gas is treated in first approximation as a homogeneous BCS state at nonzero temperature, containing both superfluid pairs and unpaired thermal atoms with a Fermi-Dirac distribution $n_F(\epsilon_{\mathbf{k},i}) = 1/[1 + \exp(\epsilon_{\mathbf{k},i}/k_B T)]$, where $\epsilon_{\mathbf{k},i} = \sqrt{(\hbar^2 k^2/2m - \mu_i)^2 + \Delta_i^2}$ is the initial spectrum, and Δ_i and μ_i are the initial gap and chemical potential, respectively. Following the quench, the initial momentum distribution of the atoms $n_{\mathbf{k}}(t=0) = n_{\mathbf{k},i}$ and pair correlation function $c_{\mathbf{k}}(t=0) = c_{\mathbf{k},i}$ are out of equilibrium and evolve according to the time-dependent BCS equations,

$$i\hbar\partial_t n_{\mathbf{k}} = \Delta c_{\mathbf{k}}^* - c_{\mathbf{k}} \Delta^*, \quad (1)$$

$$i\hbar\partial_t c_{\mathbf{k}} = (\hbar^2 k^2/m)c_{\mathbf{k}} + (1 - 2n_{\mathbf{k}})\Delta, \quad (2)$$

where a nonlinearity is caused by the gap equation $\Delta(t) = g_0 \int d^3k c_{\mathbf{k}}/(2\pi)^3$ with g_0 the coupling constant of the short-range interactions.

For temperatures well below T_c , our quench is shallow ($|\Delta_i - \Delta(t)| \ll \Delta_i$), and the cloud remains close to equilibrium. In this limit, the dynamical system (1) and (2) can be treated within linear response and the time evolution of Δ can be expressed as a Fourier transform of the amplitude-amplitude response function $\chi_{|\Delta||\Delta|}$ [40],

$$\Delta(t) - \Delta_\infty \propto \int_{2\Delta/\hbar}^{+\infty} \frac{\cos \omega t}{\omega} \chi''_{|\Delta||\Delta|}(\omega) d\omega, \quad (3)$$

where the asymptotic value $\Delta_\infty = \Delta(t \rightarrow +\infty)$ is not necessarily the equilibrium state in this integrable theory. This frequency integral covers the superposition of all excited states with energy $2\epsilon_{\mathbf{k}}$, giving rise to the collective response of $\Delta(t)$. The gapped BCS spectrum sets the lower bound $2\Delta/\hbar$, and the behavior near this pair-breaking threshold governs the long-time behavior of $\Delta(t)$. In the BCS regime ($\mu_i > 0$, which includes unitarity), the amplitude response has a square-root singularity at the continuum edge, $\chi''_{|\Delta||\Delta|} \propto 1/\sqrt{\omega - 2\Delta/\hbar}$, leading to power-law damped oscillations of the form

$$\frac{\Delta(t) - \Delta_\infty}{\Delta_i - \Delta_\infty} \underset{t \gg \tau_F}{=} A_{\text{th}} \frac{\cos(2\Delta t/\hbar + \pi/4)}{(2\Delta t/\hbar)^{\gamma_{\text{th}}}}. \quad (4)$$

Theory predicts that the amplitude A_{th} decreases with temperature, whereas the damping exponent $\gamma_{\text{th}} = 1/2$ stays constant. For larger quenches triggering nonlinear dynamics, the oscillatory form (4) can remain valid, but the oscillation frequency ω_H deviates from $2\Delta/\hbar$ [27,40].

We probe these dynamics using Bragg spectroscopy. Our experiments use atom clouds confined in an oblate harmonic potential, formed by a combination of optical and magnetic fields [40], leading to a nonuniform density

distribution. As a consequence, the pairing gap $\Delta(\mathbf{r})$, set by the local Fermi energy, $E_F(\mathbf{r}) = \hbar^2(3\pi^2 n(\mathbf{r})^{2/3})/(2m)$, varies with position \mathbf{r} across the cloud. To overcome this, we probe only a small, near-homogeneous volume of the cloud using two-photon Bragg scattering. At the end of the hold time t_h , we send in two tightly focused Bragg lasers (Fig. 1), that intersect in the center of the trapped cloud, where the density distribution is most uniform [46,68]. We define the average density in the Bragg volume $\bar{n} = \int \Omega_{\text{Br}}(\mathbf{r}) n(\mathbf{r}) d^3\mathbf{r} / \int \Omega_{\text{Br}}(\mathbf{r}) d^3\mathbf{r}$, where $\Omega_{\text{Br}}(\mathbf{r})$ is the spatially dependent two-photon Rabi frequency. In the experiments presented here, we find $\bar{n} = (0.955 \pm 0.018)n_0$, where n_0 is the peak density in the trap center, to be independent of temperature within our experimental resolution (see Supplemental Material [40]). The remaining small inhomogeneities can be accounted for in our theoretical description within the local density approximation [40]. They cause an additional damping of the oscillations, as regions oscillating at different frequencies gradually dephase.

To resonantly excite pairs with zero center-of-mass momentum, we set the frequency difference between the two lasers to half of the atomic recoil [$\hbar\omega_r/2 = \hbar^2 q^2/(4m)$] [46,47]. Bragg scattered pairs begin moving with a velocity $\hbar\mathbf{q}/(2m)$, where $\mathbf{q} = \mathbf{k}_a - \mathbf{k}_b$ is the difference of the wave vectors of the two Bragg lasers. We use $q \simeq 4k_F$ to ensure that $\hbar\omega$ is large compared to E_F , and the Bragg pulse duration ($t_B = 50 \mu\text{s}$) provides good spectral resolution, while remaining 3 to 4 times shorter than the typical oscillation period ($\tau_H = 2\pi/\omega_H$) so the oscillations remain visible. We estimate that the observed oscillation magnitude is reduced by less than 15% due to this time averaging [40].

The resulting center-of-mass displacement $S = \Delta X_{\text{c.m.}}$ following time-of-flight expansion is proportional to the momentum transferred to the atoms by the Bragg lasers [40], hence to the imaginary part of density-density response function $\chi''_{nn}(\omega_r/2, q = 4k_F)$ [68]. At large q , χ''_{nn} has a sharp peak at the continuum threshold [Fig. 1(b)], which coincides approximately with the pair recoil frequency [69,70]. Both the height and energy of this peak are sensitive to variations in Δ . When $t_B \ll \tau_H$, the Higgs oscillations are approximately stationary during the Bragg pulse and the time-dependent Bragg response can be written as

$$\chi''_{nn}(\omega, q, t) \approx \chi''_{nn}(\omega, q; \Delta_i) + \frac{d\chi''_{nn}}{d\Delta} [\Delta(t) - \Delta_i]. \quad (5)$$

Our Bragg frequency $\omega = \omega_r/2$ sits just on the high-energy slope of the threshold peak [40], where χ''_{nn} is very sensitive to variations of Δ . Experimentally, we observe that the Bragg response at $\omega = \omega_r/2$ shows a strong dependence on the condensate fraction, reflecting the temperature dependence of the spectral weight of this threshold peak [40].

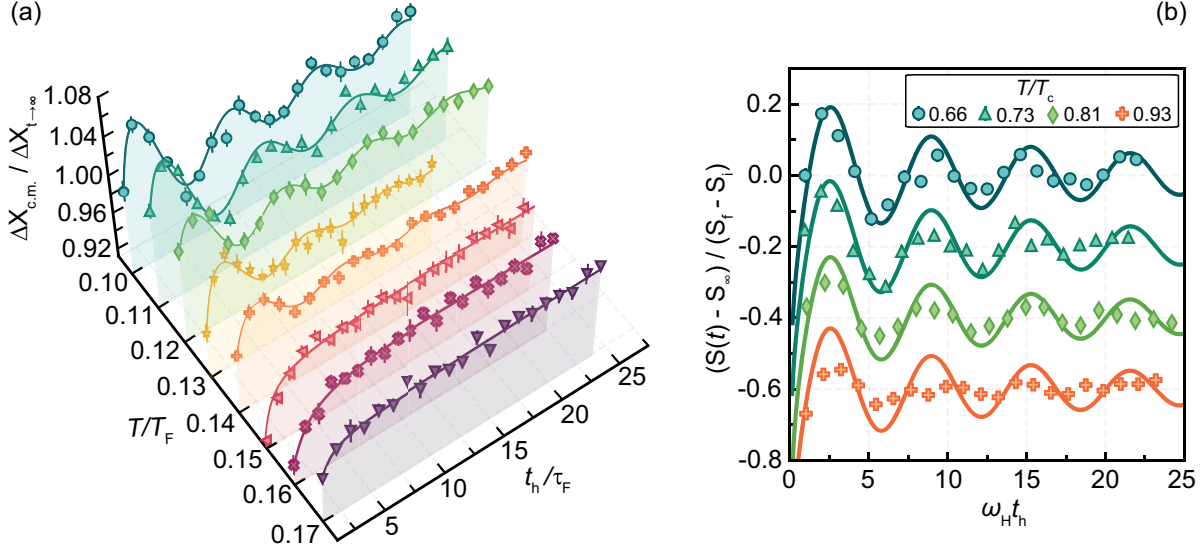


FIG. 2. (a) Bragg response (center of mass displacement S), relative to the asymptotic response S_∞ ($t \rightarrow \infty$), as function of hold time after the quench for a selection of (final) equilibrium cloud temperatures. Points are the experimental measurements and solid lines are fits to the data of a power-law damped sinusoidal function (see text). (b) Comparison with time-dependent BCS theory including experimental effects [40]. The experimental points are shown as a function of $\omega_H t_h$ and T/T_c using the fitted value of $\hbar\omega_H/E_F$ and the estimated value $T_{c,i}/T_F \approx 0.15$ [72] at $1/k_F a = -0.18$. The Bragg signal $S(t) - S_\infty$ is scaled to its variation $S_f - S_i$ under an adiabatic sweep of the scattering length, which we measured independently, and the theoretical curves are offset by the delay accumulated during the ramp [40]. The curves for different values of T are vertically offset by 0.2 for readability.

Armed with this capability, we use local Bragg scattering as a sensitive, temporally resolved probe for oscillations of the order parameter. Figure 2 shows examples of the measured Bragg response, as a function of hold time t_h , in units of the local Fermi time $\tau_F = \hbar/E_F$, for a range of temperatures [40,71]. A damped oscillation is clear in the Bragg response of the colder clouds, giving a direct signature of the Higgs oscillations. The magnitude of the oscillations decreases for warmer clouds, until nonoscillatory behavior is observed for $T \gtrsim 0.15T_F$. Also shown are fits of the data to a function of the form $S(t) = A_{\text{ex}} \cos(\omega_H t + \phi)/t^\gamma + S_\infty$, where A_{ex} , ω_H , ϕ , γ , and S_∞ are fit parameters that characterize the oscillations.

To compare our experimental measurements to theory, we obtain the asymptotic Bragg response S_∞ ($t \rightarrow \infty$) and then separately measure the responses S_i and S_f at thermal equilibrium with the initial and final scattering lengths. From these we construct the ratio $[S(t) - S_\infty]/(S_f - S_i)$, which we directly compare to the theoretical equivalent $[\Delta(t) - \Delta_\infty]/(\Delta_f - \Delta_i)$. The advantage of comparing these quantities is that they do not depend on the experimental sensitivity $d\chi''_{nm}/d\Delta$ or the offset in the experimental data due to the normal phase response $\chi_{nm}(T > T_c)$, which is not captured in BCS theory. Note that the experimental and theoretical temperatures are scaled by the respective critical temperatures of the initial clouds $T_{c,i}$. In Fig. 2(b) we see good agreement in the dynamics at short times and lower temperatures; however, at later times, the experimental signal decays faster than theoretically predicted. This is emphasized in

Fig. 3(b), which shows the root-mean-square amplitude $A_{\text{rms}} = \sqrt{[1/(t_2 - t_1)] \int_{t_1}^{t_2} dt [S(t) - S_\infty]^2 / (S_f - S_i)^2}$, a quantity that does not depend on any of the fitted parameters apart from S_∞ . While the theory overestimates the magnitude of the oscillations by only 10%–20% in the short time window $1 \leq t/\tau_H \leq 10$, the overestimate grows to roughly a factor of 2 at later times $3 \leq t/\tau_H \leq 20$. Although the quicker decay of the experimental signal may be due to experimental effects other than those we have taken into account in our realistic theory [40], we note that the prediction of a slow power-law decay is based on integrable, collisionless theories [27] and may be violated at long times, in particular, at times comparable to the quasiparticle collision time [22].

From the fits to the experimental data we extract the oscillation frequency ω_H and damping exponent γ . Figure 3(a) shows $\hbar\omega_H/2E_F$ versus temperature for data points taken in the $|F = 1/2, m_F = \pm 1/2\rangle$ hyperfine states ($= |1\rangle - |2\rangle$, blue circles) and $|F = 1/2, m_F = +1/2\rangle - |F = 3/2, m_F = -3/2\rangle$ hyperfine states ($= |1\rangle - |3\rangle$, green squares) and confronts the data to a selection of previous measurements and calculations of the pairing gap Δ . Theoretically, we expect $\hbar\omega_H$ to provide a lower bound on 2Δ and to approach this value at low temperatures when our quench is in the shallow regime. Our measurements lie mostly in the range $0.4 \lesssim \hbar\omega_H/2E_F \lesssim 0.5$. At low temperature, they are in good agreement with previous measurements of 2Δ [36,68,73], as well as beyond mean-field predictions [74,75] and quantum Monte Carlo calculations [76,77]. Although Δ is expected to vanish with a critical exponent of

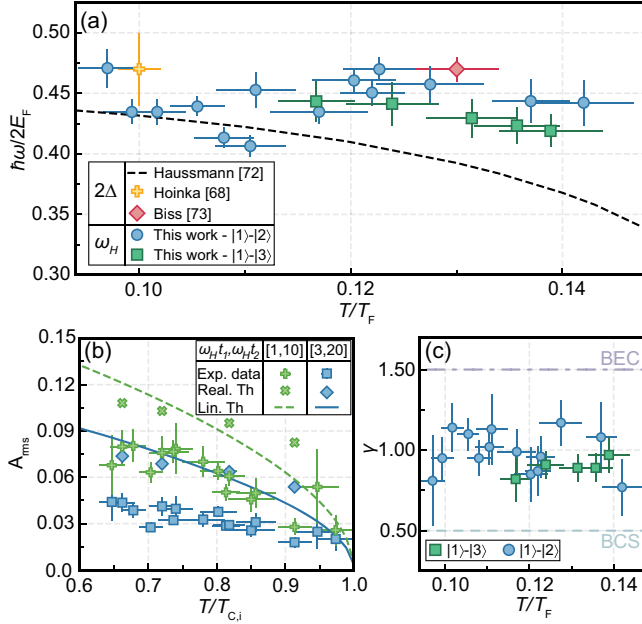


FIG. 3. (a) Frequency of the Higgs oscillation ω_H versus the normalized temperature T/T_F , along with previous measurements and a theoretical calculation (dashed line) of 2Δ . Blue circles and green squares represent measurements using different combinations of internal states (but for the same interaction quench) [40]. (b) The root-mean-square magnitude of the oscillations, measured experimentally (symbols with error bars), predicted analytically from the amplitude response function (solid line), and obtained from a numerical model taking into account experimental imperfections (symbols without error bars) [40]. (c) The fitted damping exponent γ of the Higgs oscillation.

$\nu \simeq 0.62$ at T_c [78], we do not observe a noticeable reduction of ω_H in the temperature range we probe.

Figure 3(c) shows the fitted damping exponents γ , which all lie close to unity. While the uncertainties in γ are relatively large, our measurements are not consistent with either the BEC or BCS exponents and display no obvious temperature dependence. The average of our measured damping coefficients is $\bar{\gamma} = 0.98 \pm 0.15$. This is significantly above the theoretical prediction of $\gamma_{th} = 0.50 \pm 0.02$ [40], where we take into account the inhomogeneous density and the finite experimental time window. These effects lead to compensating shifts on the BCS prediction $\gamma_{th} = 1/2$, resulting in a correction that is small compared to the difference between BCS and BEC limits.

We note that fitting an exponentially decaying cosine function to the experimental data gives a statistically indistinguishable quality of fit such that we cannot rule out exponential decay or that γ is affected by other ergodic processes such as quasiparticle collisions. In the vicinity of T_c , the local density approximation may also break down for describing delocalized pairs. Effects of the inhomogeneity of the cloud may thus become enhanced even in the nearly uniform region probed by our Bragg beams.

Fifty years after their prediction [22], we present the direct observation of amplitude oscillations in a weakly excited Fermi superfluid. Using Bragg spectroscopy, we probe the real-time dynamics at unitarity, in qualitative agreement with time-dependent BCS theory at low temperatures. Our Letter opens a wide avenue of research, with possible direct extensions to the BCS and BEC regimes, different quench regimes [27], or dynamical crossings of the phase transition [37–39]. Our Letter also opens pathways to investigate ergodic evolution and the possibility of achieving preequilibrated states in strongly interacting quantum matter.

We thank Y. Castin, F. Dalfovo, M. Davis, N. Navon, C. Sa de Melo, S. Stringari, and M. Zwierlein for valuable discussions and comments on the manuscript. This work was supported by the ARC Centre of Excellence for Future Low-Energy Electronics Technologies. V.C. acknowledges financial support from Provincia Autonoma di Trento, the Italian MIUR under the PRIN2017 project CENTraL and the National Science Foundation under Grant No. NSF PHY-1748958. S.M. acknowledges funding from the ANR-21-CE47-0009 Quantum-SOPHA project. D.J.M.A.-B. and S.J.J.M.F.K. acknowledge financial support from the Dutch Ministry of Economic Affairs and Climate Policy (EZK), as part of the Quantum Delta NL program, and by the Netherlands Organisation for Scientific Research (NWO) under Grants No. 680.92.18.05 and No. 680.47.623.

- [1] S. Sachdev, *Quantum Phase Transitions*, 2nd ed. (Cambridge University Press, Cambridge, England, 2011).
- [2] N. Bogoliubov, *J. Phys.* **11**, 23 (1947).
- [3] P. W. Anderson, *Phys. Rev.* **112**, 1900 (1958).
- [4] T. Repplinger, S. Klimin, M. Gélédan, J. Tempere, and H. Kurkjian, *Phys. Rev. B* **107**, 014504 (2023).
- [5] P. W. Higgs, *Phys. Rev. Lett.* **13**, 508 (1964).
- [6] D. Pekker and C. Varma, *Annu. Rev. Condens. Matter Phys.* **6**, 269 (2015).
- [7] R. Shimano and N. Tsuji, *Annu. Rev. Condens. Matter Phys.* **11**, 103 (2020).
- [8] U. Bissbort, S. Götze, Y. Li, J. Heinze, J. S. Krauser, M. Weinberg, C. Becker, K. Sengstock, and W. Hofstetter, *Phys. Rev. Lett.* **106**, 205303 (2011).
- [9] M. Endres, T. Fukuhara, D. Pekker, M. Cheneau, P. Schauss, C. Gross, E. Demler, S. Kuhr, and I. Bloch, *Nature (London)* **487**, 454 (2012).
- [10] T. M. Hoang, H. M. Bharath, M. J. Boguslawski, M. Anquez, B. A. Robbins, and M. S. Chapman, *Proc. Natl. Acad. Sci. U.S.A.* **113**, 9475 (2016).
- [11] J. Léonard, A. Morales, P. Zupancic, T. Donner, and T. Esslinger, *Science* **358**, 1415 (2017).
- [12] J. Hertkorn, F. Böttcher, M. Guo, J. N. Schmidt, T. Langen, H. P. Büchler, and T. Pfau, *Phys. Rev. Lett.* **123**, 193002 (2019).

- [13] A. Jain, M. Krautloher, J. Porras, G. H. Ryu, D. P. Chen, D. L. Abernathy, J. T. Park, A. Ivanov, J. Chaloupka, G. Khaliullin, B. Keimer, and B. J. Kim, *Nat. Phys.* **13**, 633 (2017).
- [14] R. Matsunaga, Y. I. Hamada, K. Makise, Y. Uzawa, H. Terai, Z. Wang, and R. Shimano, *Phys. Rev. Lett.* **111**, 057002 (2013).
- [15] V. V. Zavjalov, S. Autti, V. B. Eltsov, P. J. Heikkinen, and G. E. Volovik, *Nat. Commun.* **7**, 10294 (2016).
- [16] A. Behrle, T. Harrison, J. Kombe, K. Gao, M. Link, J.-S. Bernier, C. Kollath, and M. Köhl, *Nat. Phys.* **14**, 781 (2018).
- [17] I. M. Khalatnikov, *An Introduction to the Theory of Superfluidity* (Perseus Publishing, Cambridge, MA, 2000).
- [18] T. Cea, C. Castellani, G. Seibold, and L. Benfatto, *Phys. Rev. Lett.* **115**, 157002 (2015).
- [19] V. A. Andrianov and V. N. Popov, *Theor. Math. Phys.* **28**, 829 (1976).
- [20] H. Kurkjian, S. N. Klimin, J. Tempere, and Y. Castin, *Phys. Rev. Lett.* **122**, 093403 (2019).
- [21] R. G. Scott, F. Dalfovo, L. P. Pitaevskii, and S. Stringari, *Phys. Rev. A* **86**, 053604 (2012).
- [22] A. F. Volkov and S. M. Kogan, *Sov. J. Exp. Theor. Phys.* **38**, 1018 (1974), <http://jetp.ras.ru/cgi-bin/e/index/e/38/5/p1018?a=list>.
- [23] E. A. Yuzbashyan, O. Tsypliyatyev, and B. L. Altshuler, *Phys. Rev. Lett.* **96**, 097005 (2006).
- [24] V. Gurarie, *Phys. Rev. Lett.* **103**, 075301 (2009).
- [25] B. Liu, H. Zhai, and S. Zhang, *Phys. Rev. A* **93**, 033641 (2016).
- [26] J. Tokimoto, S. Tsuchiya, and T. Nikuni, *J. Low Temp. Phys.* **187**, 765 (2017).
- [27] E. A. Yuzbashyan, M. Dzero, V. Gurarie, and M. S. Foster, *Phys. Rev. A* **91**, 033628 (2015).
- [28] R. J. Lewis-Swan, D. Barberena, J. R. K. Cline, D. J. Young, J. K. Thompson, and A. M. Rey, *Phys. Rev. Lett.* **126**, 173601 (2021).
- [29] D. J. Young, A. Chu, E. Y. Song, D. Barberena, D. Wellnitz, Z. Niu, V. M. Schäfer, R. J. Lewis-Swan, A. M. Rey, and J. K. Thompson, *Nature (London)* **625**, 679 (2024).
- [30] K. Katsumi, N. Tsuji, Y. I. Hamada, R. Matsunaga, J. Schneeloch, R. D. Zhong, G. D. Gu, H. Aoki, Y. Gallais, and R. Shimano, *Phys. Rev. Lett.* **120**, 117001 (2018).
- [31] H. Chu, M.-J. Kim, K. Katsumi, S. Kovalev, R. D. Dawson, L. Schwarz, N. Yoshikawa, G. Kim, D. Putzky, Z. Z. Li *et al.*, *Nat. Commun.* **11**, 1793 (2020).
- [32] R. Sooryakumar and M. V. Klein, *Phys. Rev. Lett.* **45**, 660 (1980).
- [33] M.-A. Méasson, Y. Gallais, M. Cazayous, B. Clair, P. Rodière, L. Cario, and A. Sacuto, *Phys. Rev. B* **89**, 060503(R) (2014).
- [34] R. Grasset, Y. Gallais, A. Sacuto, M. Cazayous, S. Mañas-Valero, E. Coronado, and M.-A. Méasson, *Phys. Rev. Lett.* **122**, 127001 (2019).
- [35] M. Greiner, C. A. Regal, and D. S. Jin, *Phys. Rev. Lett.* **94**, 070403 (2005).
- [36] A. Schirotzek, Y.-i. Shin, C. H. Schunck, and W. Ketterle, *Phys. Rev. Lett.* **101**, 140403 (2008).
- [37] M. W. Zwierlein, C. H. Schunck, C. A. Stan, S. M. F. Raupach, and W. Ketterle, *Phys. Rev. Lett.* **94**, 180401 (2005).
- [38] T. Harrison, M. Link, A. Behrle, K. Gao, A. Kell, J. Kombe, J.-S. Bernier, C. Kollath, and M. Köhl, *Phys. Rev. Res.* **3**, 023205 (2021).
- [39] P. Dyke, A. Hogan, I. Herrera, C. C. N. Kuhn, S. Hoinka, and C. J. Vale, *Phys. Rev. Lett.* **127**, 100405 (2021).
- [40] See Supplemental Material at <http://link.aps.org/supplemental/10.1103/PhysRevLett.132.223402> for additional information about the experimental methods and a detailed discussion of the theoretical analysis, which includes Refs. [41–66].
- [41] N. L. Smith, W. H. Heathcote, G. Hechenblaikner, E. Nugent, and C. J. Foot, *J. Phys. B* **38**, 223 (2005).
- [42] S. P. Rath, T. Yefsah, K. J. Günter, M. Cheneau, R. Desbuquois, M. Holzmann, W. Krauth, and J. Dalibard, *Phys. Rev. A* **82**, 013609 (2010).
- [43] P. Dyke, K. Fenech, T. Peppler, M. G. Lingham, S. Hoinka, W. Zhang, S.-G. Peng, B. Mulkerin, H. Hu, X.-J. Liu, and C. J. Vale, *Phys. Rev. A* **93**, 011603(R) (2016).
- [44] G. Zürn, T. Lompe, A. N. Wenz, S. Jochim, P. S. Julienne, and J. M. Hutson, *Phys. Rev. Lett.* **110**, 135301 (2013).
- [45] M. J. H. Ku, A. T. Sommer, L. W. Cheuk, and M. W. Zwierlein, *Science* **335**, 563 (2012).
- [46] C. Carcy, S. Hoinka, M. G. Lingham, P. Dyke, C. C. N. Kuhn, H. Hu, and C. J. Vale, *Phys. Rev. Lett.* **122**, 203401 (2019).
- [47] M. G. Lingham, K. Fenech, S. Hoinka, and C. J. Vale, *Phys. Rev. Lett.* **112**, 100404 (2014).
- [48] G. Veeravalli, E. Kuhnle, P. Dyke, and C. J. Vale, *Phys. Rev. Lett.* **101**, 250403 (2008).
- [49] C. A. Regal, M. Greiner, and D. S. Jin, *Phys. Rev. Lett.* **92**, 040403 (2004).
- [50] C. Chin, R. Grimm, P. Julienne, and E. Tiesinga, *Rev. Mod. Phys.* **82**, 1225 (2010).
- [51] G. C. Strinati, P. Pieri, G. Röpke, P. Schuck, and M. Urban, *Phys. Rep.* **738**, 1 (2018).
- [52] W. H. Press, B. P. Flannery, S. A. Teukolsky, W. T. Vetterling *et al.*, *Numerical Recipes* (Cambridge University Press, Cambridge, England, 1989), Vol. 3.
- [53] M. Holland, S. J. J. M. F. Kokkelmans, M. L. Chiofalo, and R. Walser, *Phys. Rev. Lett.* **87**, 120406 (2001).
- [54] S. J. J. M. F. Kokkelmans, J. N. Milstein, M. L. Chiofalo, R. Walser, and M. J. Holland, *Phys. Rev. A* **65**, 053617 (2002).
- [55] R. A. Barankov, L. S. Levitov, and B. Z. Spivak, *Phys. Rev. Lett.* **93**, 160401 (2004).
- [56] L. Pitaevskii and S. Stringari, *Bose-Einstein Condensation and Superfluidity* (Oxford University Press, New York, 2016), Vol. 164.
- [57] M. Marini, F. Pistolesi, and G. Strinati, *Eur. Phys. J. B* **1**, 151 (1998).
- [58] A. Perali, P. Pieri, and G. C. Strinati, *Phys. Rev. A* **68**, 031601(R) (2003).
- [59] L. Salasnich, N. Manini, and A. Parola, *Phys. Rev. A* **72**, 023621 (2005).
- [60] M. L. Chiofalo, S. J. J. M. F. Kokkelmans, J. N. Milstein, and M. J. Holland, *Phys. Rev. Lett.* **88**, 090402 (2002).
- [61] R. Haussmann and W. Zwerger, *Phys. Rev. A* **78**, 063602 (2008).
- [62] T.-L. Ho, *Phys. Rev. Lett.* **92**, 090402 (2004).

- [63] A. Perali, P. Pieri, and G. C. Strinati, *Phys. Rev. Lett.* **93**, 100404 (2004).
- [64] W. Krauth, *Statistical Mechanics Algorithms and Computations* (Oxford University Press, Oxford, 2006).
- [65] G. M. Bruun and B. R. Mottelson, *Phys. Rev. Lett.* **87**, 270403 (2001).
- [66] A. Minguzzi, G. Ferrari, and Y. Castin, *Eur. Phys. J. D* **17**, 49 (2001).
- [67] J.-P. Blaizot and G. Ripka, *Quantum Theory of Finite Systems* (MIT Press, Cambridge, MA, 1985).
- [68] S. Hoinka, P. Dyke, M. G. Lingham, J. J. Kinnunen, G. M. Bruun, and C. J. Vale, *Nat. Phys.* **13**, 943 (2017).
- [69] R. Combescot, M. Y. Kagan, and S. Stringari, *Phys. Rev. A* **74**, 042717 (2006).
- [70] H. Kurkjian, J. Tempere, and S. N. Klimin, *Sci. Rep.* **10**, 11591 (2020).
- [71] Note that the temperature of the cloud was measured after the quench at unitarity. This includes some heating due to the nonadiabatic experimental quench, which is not accounted for by BCS theory.
- [72] R. Haussmann, W. Rantner, S. Cerrito, and W. Zwerger, *Phys. Rev. A* **75**, 023610 (2007).
- [73] H. Biss, L. Sobirey, N. Luick, M. Bohlen, J. J. Kinnunen, G. M. Bruun, T. Lompe, and H. Moritz, *Phys. Rev. Lett.* **128**, 100401 (2022).
- [74] R. Haussmann, M. Punk, and W. Zwerger, *Phys. Rev. A* **80**, 063612 (2009).
- [75] L. Pisani, P. Pieri, and G. C. Strinati, *Phys. Rev. B* **98**, 104507 (2018).
- [76] A. Bulgac, J. E. Drut, and P. Magierski, *Phys. Rev. Lett.* **96**, 090404 (2006).
- [77] A. Gezerlis and J. Carlson, *Phys. Rev. C* **77**, 032801(R) (2008).
- [78] S. Diehl, S. Floerchinger, H. Gies, J. Pawlowksi, and C. Wetterich, *Ann. Phys. (Berlin)* **522**, 615 (2010).